Route to Three-Dimensional Metallized Microstructures Using Cross-Linkable Epoxide SU-8

Yun-Sheng Chen,[†] Amir Tal,[†] and Stephen M. Kuebler*[,†,‡]

Department of Chemistry and CREOL, The College of Optics and Photonics, University of Central Florida, Orlando, Florida 32816

Received April 20, 2007
Revised Manuscript Received June 18, 2007

Versatile approaches for three-dimensional (3D) submicrometer fabrication are needed to advance the emerging technologies of micro- and nanoscale fluidics, photonics, and electromechanical systems (MEMS). Patterning 3D metallic and conductive structures is of particular interest for preparing functional devices having electronic, optical, and mechanical function.[1] Multiphoton direct laser writing (DLW) is a flexible technique for creating micrometer-scale polymeric structures having virtually any 3D shape.[2] It has been shown that metallized 3D micro-structures can be created by fabricating a polymeric scaffold using multiphoton DLW and then depositing metal onto the structure by surface-catalyzed electroless deposition.[3] Thus far, processes have only been reported for metallizing acrylate-based microstructures. Yet, acrylates are comparatively poor materials for microfabrication because they shrink substantially upon polymerization, compromising structural form, integrity, and adhesion to a supporting surface.[4] The multifunctional epoxide SU-8 is better suited for microfabrication because it shrinks little upon polymerization (<10%),[5] the monomer is a solid, and the cross-linked material is mechanically robust, chemically resistant, and optically transparent.[6] Consequently, SU-8 is increasingly used for microdevice fabrication.[7] Here, we report a method for creating high-quality silvered polymeric 3D microstructures, like those shown in Figure 1, based on multiphoton DLW using SU-8 followed by surface functionalization and electroless metal deposition.

Polymeric microstructures were created by multiphoton DLW in ∼50 μm thick slabs of SU-8 pre-polymer spin-coated onto glass or silicon substrates.[2(c),8] Metallized structures were created by (1) functionalizing the surface of an SU-8 microstructure with alkylamino groups, (2) binding gold nanoparticles (Au-NPs) at the aminated sites, and (3) depositing Ag onto the primed polymeric scaffold using electroless metallization chemistry.[3(d),9] bis-Amino-terminated *n*-alkanes were chosen for functionalizing the polymeric surface, reasoning that one amino group could bind covalently via nucleophilic attack at unreacted epoxide moeities, leaving the second amino group available for coordinating Au-NPs. Au-NPs were bound to the aminated surface by treating the sample with a colloidal suspension of citrate-capped Au-NPs[10] or by synthesizing Au-NPs directly at the surface via hydride reduction of coordinated Au(III). Ag was deposited by immersing a Au-NP-functionalized structure for varying periods into an aqueous buffered bath containing silver lactate (5.6 mM or 33 mM), hydroquinone, and in some cases gum arabic. Additional information concerning the formulations and processing conditions is available in the Supporting Information.

The silvered SU-8 microstructure shown in Figure 1 was produced by immersing a Au-NP functionalized sample in a $[Ag^+] = 33$ mM bath containing gum arabic for 14 min. Figure 1A−C contains scanning electron microscopy (SEM) images that illustrate that high-quality microporous structures can be created by this approach. The structure consists of layers of parallel logs, each having a total length of 62.4 μm and spaced within a layer by $a = 2.6$ μm. The layers are separated vertically by $c/4 = 1.0$ μm. Logs in immediately adjacent layers are oriented perpendicularly. Logs are thus parallel in alternate layers but offset laterally by $a/2$. The resulting structure has face-centered-tetragonal (FCT) symmetry with a basis consisting of two crossed logs.[11] The unit cell has base length and width $a\sqrt{2} = 3.7$ μm and height $c = 4.0$ μm. The overall structure has base

* Corresponding author. E-mail: kuebler@mail.ucf.edu.
† CREOL, The College of Optics and Photonics, University of Central Florida.
‡ Department of Chemistry, University of Central Florida.

(1) (a) Jiang, L. M.; Liu, Z. F.; Tang, J.; Zhang, L.; K. S.; Tian, Z. Q.; Liu, P. K.; Sun, L. N.; Tian, Z. W. *J. Electroanal. Chem.* **2005**, *581*, 153. (b) Smoukov, S. K.; Bishop, K. J. M.; Campbell, C. J.; Grzybowski, B. A. *Adv. Mater.* **2005**, *17*, 751. (c) Yoon, Y.-K.; Park, J.-H.; Allen, M. G. *J. Microelectromech. Syst.* **2006**, *15*, 1121. (d) Kozlov, M. E.; Murthy, N. S.; Udod, I.; Khayrullin, I. I.; Baughman, R. H.; Zakhidov, A. A. *Appl. Phys. A: Mater. Sci. Process.* **2007**, *86*, 421.

(2) (a) Wu, E. S.; Strickler, J. H.; Harrell, W. R.; Webb, W. W. *Proc. SPIE* **1992**, *1674*, 776. (b) Maruo, S.; Nakamura, O.; Kawata, S. *Opt. Lett.* **1997**, *22*, 132. (c) Kuebler, S. M.; Rumi, M. In *Encyclopedia of Modern Optics*; Guenther, R. D., Steel, D. G., Bayvel, L., Eds.; Elsevier: Oxford, U.K., 2004; p 189. (d) Li, L.; Fourkas, J. T. *Mater. Today* **2007**, *10*, 30.

(3) (a) Hill, R. T.; Lyon, L. J.; Allen, R.; Stevenson, K. J.; Shear, J. B. *J. Am. Chem. Soc.* **2005**, *127*, 10707. (b) Farrer, M. R.; LaFratta, C. N.; Li, L.; Praino, J.; Naughton, M. J.; Saleh, B. E. A.; Teich, M. C.; Fourkas, J. T. *J. Am. Chem. Soc.* **2006**, *128*, 1796. (c) Chen, Y.-S.; Tal, A.; Torrance, D. B.; Kuebler, S. M. *Adv. Funct. Mater.* **2006**, *16*, 1739. (d) Formanek, F.; Takeyasu, N.; Tanaka, T.; Chiyoda, K.; Ishikawa, A.; Kawata, S. *Appl. Phys. Lett.* **2006**, *88*, 083110.

(4) Odian, G. *Principles of Polymerization*, 4th ed.; Wiley: New York, 2004.

(5) Guerin, L. J.; Bossel, M.; Demierre, M.; Calmes, S.; Renaud, P. *Proceedings of the International Conference on Solid-State Sensors and Actuators (Transducers '97)*, Chicago, June 16−19, 1997; IEE Electron Devices Society: Piscataway, NJ, 1997; Vol. 2, p 1419.

(6) (a) Lee, K. Y.; LaBianca, N.; Rishton, S. A.; Zolgharnain, S.; Gelorme, J. D.; Shaw, J.; Chang, T. H.-P. *J. Vac. Sci. Technol., B* **1995**, *13*, 3012. (b) Lorenz, H.; Despont, M.; Fahrni, N.; LaBianca, N.; Renaud, P.; Vettiger, P. *J. Micromech. Microeng.* **1997**, *7*, 121.

(7) (a) Llobera, A.; Seidemann, V.; Plaza, J. A.; Cadarso, V. J.; Büttgenbach, S. *J. Microelectromech. Syst.* **2007**, *16*, 111−121. (b) Chung, C. K.; Hong, Y. Z. *J. Micromech. Microeng.* **2007**, *17*, 207. (c) Rajaraman, S.; Choi, S.-O.; Shafer, R. H.; Ross, J. D.; Vukasinovic, J.; Choi, Y.; DeWeerth, S. P.; Glezer, A.; Allen, M. G. *J. Micromech. Microeng.* **2007**, *17*, 163.

(8) Teh, W. H.; Dürig, U.; Drechsler, U.; Smith, C. G.; Güntherodt, H.-J. *J. Appl. Phys.* **2005**, *97*, 054907.

(9) Henry, A. C.; McCarley, R. L. *J. Phys. Chem. B* **2001**, *105*, 8755.

(10) Lee, P. C.; Meisel, D. *J. Phys. Chem.* **1982**, *86*, 3391.

(11) Ho, K. M.; Chan, C. T.; Soukoulis, C. M.; Biswas, R.; Sigalas, M. *Solid State Commun.* **1994**, *89*, 413.

10.1021/cm0710812 CCC: $37.00
Published on Web 07/04/2007

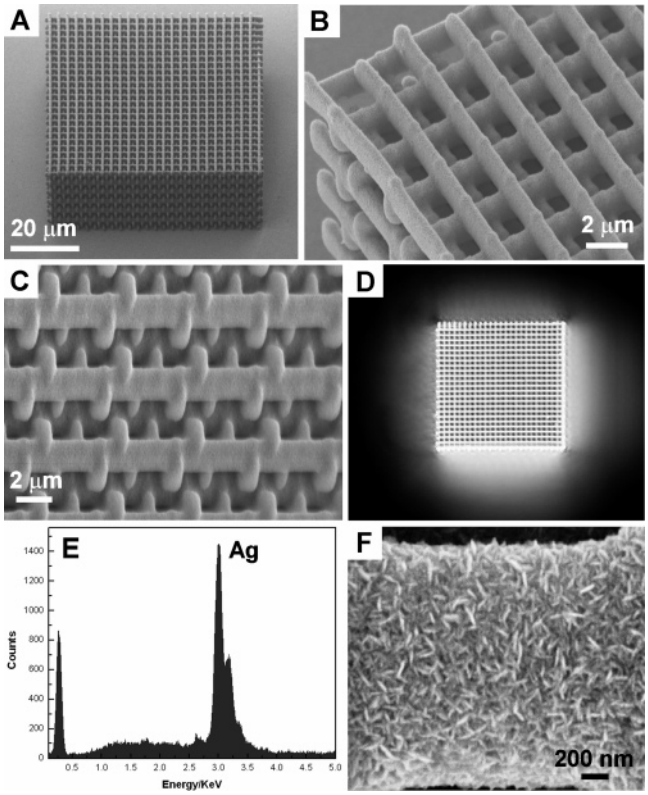

Figure 1. Silvered polymeric "stack-of-logs" microstructure supported on a glass coverslip substrate. (A−C) SEM images of the metallized structure. (D) Optical reflection microscopy image showing that the silvered structure is highly reflective. (E) Energy-dispersive X-ray spectrum of the structure. The dominant peak at 3.0 keV proves that the structure is coated with Ag metal. (F) High-magnification SEM image of the structure showing that Ag deposits as rice-shaped NPs when the silvering medium contains $[Ag^+] = 33$ mM.

area of $(62.4\ \mu m)^2$ and height just over 24 μm (6 unit cells). Infrared optical properties specific to this structure-type will be reported elsewhere.

Energy dispersive X-ray analysis of the surface (Figure 1E) yielded a dominant peak near 3.0 keV, which confirms that the exterior is coated with metallic Ag. Control experiments show that Ag is only deposited when the epoxide structure is subjected to both surface amination and Au-NP functionalization, which is consistent with the surface-bound Au-NPs catalyzing initial metal deposition.[12] As a result, the epoxide structure is initially transparent at visible wavelengths, but upon silvering it becomes highly reflective (Figure 1D). In contrast, the substrate remains dull because the amination chemistry does not functionalize the glass substrate. The method provides a means then for selectively silvering SU-8 microstructures while leaving the surrounding chemically inactive materials unaltered. The optical reflectivity of silvered SU-8 at visible and infrared wavelengths was measured using uniform thin films and found to exceed 90% for Ag layers of *ca.* 100 nm or thicker. Imaging the surface at higher magnification (Figure 1F) reveals that Ag deposits under these conditions in the form of rice-shaped crystallites that average 150 nm in length and 50 nm in width.

(12) (a) Sacher, E.; Pireaux, J. J.; Kowalczyk, S. P. *Metallization of Polymers*; American Chemical Society: Washington, D.C., 1990. (b) *Metallized Plastics 5 & 6: Fundamental and Applied Aspects*; Mittal, K. L., Ed.; VSP: Utrecht, The Netherlands, 1998.

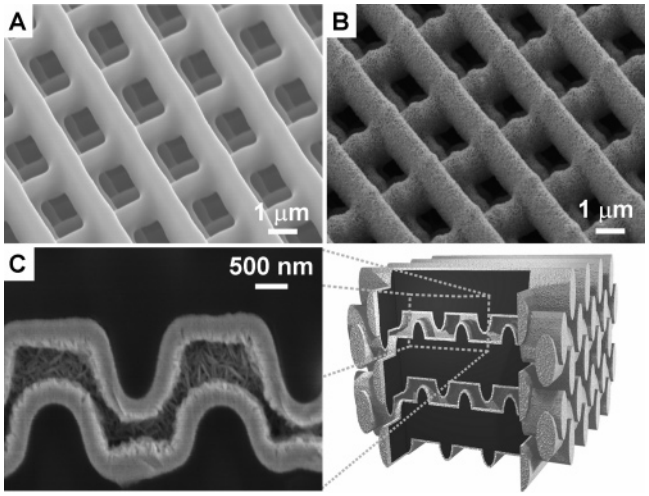

Figure 2. SEM images illustrating that the process deposits Ag conformally onto SU-8 microstructures, even for higly microporous lattices. (A) FCT microstructure prior to silvering. (B) FCT microstructure following Ag deposition. (C) Cross-sectional image (left) produced by ion-milling the silvered microstructure shown in Figure 2B normal to the long axis of the stacked logs. The schematic at right illustrates the cut-out produced by ion milling, the view direction, and how milling the FCT lattice produces the cross-sectional image shown at left.

The process conformally metallizes the entire polymeric surface, even deep within a microporous structure, without occluding internal voids. Images A and B in Figure 2 are SEM images of a structure prior and subsequent to silvering, respectively, which illustrate that the overall form of the lattice is retained upon metallization. Parallel logs in the interior of the structure are easily seen upon close inspection of Figures 1B and 2B, and one can also see completely through the lattice along the structure's edge in Figure 1B.

Conformal deposition is further confirmed from the cross-sectional SEM images of Figure 2C. The cross-section was obtained by ion milling into the interior of a silvered structure. The regions of cross-linked polymer appear dark, whereas the silvered layer appears bright. The bright corrugated strips result from the cross-section of Ag-covered logs oriented parallel to the view direction. The rice-shaped Ag particles visible between the corrugated strips are actually covering the surface of a log oriented perpendicular to the view direction and whose center lies behind the image plane. The interior of the corrugated Ag path appears denser than the rice-shaped particles on the surface, but this is likely the result of thermal annealing occurring during ion milling. Bearing in mind that the metal layer thickness may be altered by milling-induced annealing, we estimate the metal layer thickness from the image to be approximately 200−300 nm. These values are consistent with separate measurements obtained by surface profilometry of acid-etched, silvered thin films.[3c] Thicker metal layers can be obtained by simply lengthening the time for which samples are immersed in the silvering bath.

The nanoscale morphology of deposited Ag was found to be controllable through concentration of Ag^+ in the bath and the presence or absence of gum arabic. Figure 3 presents SEM images of Ag deposited onto two SU-8 films that were spin-coated, cured, and then metallized using silvering baths containing gum arabic and $[Ag^+] = 33$ mM or 5.6 mM. High Ag^+ concentration generated the rice-shaped morphology

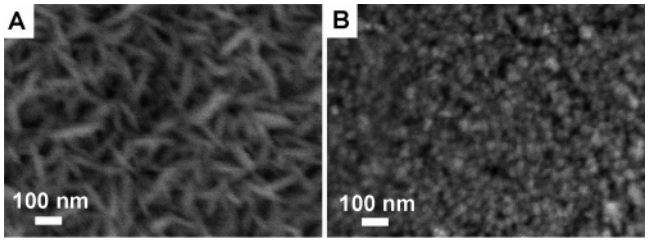

Figure 3. SEM images of silvered SU-8 films showing that the nanoscale morphology depends on $[Ag^+]$ for the process reported here. (A) High $[Ag^+]$ (33 mM) favors formation of rice-shaped particles (see also Figures 1F and 2C), whereas (B) low $[Ag^+]$ (5.6 mM) favors formation of spheroidal crystallites.

seen in Figure 3A (and Figures 1F and 2C). In contrast, lower Ag^+ concentration produced Ag grains having a nearly spheroidal morphology, as in Figure 3B, with grain diameter varying between 25 and 100 nm. The morphology appears to transition between these two extremes at $[Ag^+] \approx 17$ mM. In the absence of gum arabic, Ag deposited more quickly, but selectivity toward deposition on the polymer was poorer and only the rice-shaped morphology was obtained. Four-point probe measurements confirm that Ag deposited under any of these conditions is conductive, $\sigma \geq 1\ \Omega^{-1}\ cm^{-1}$. The highest conductivity, $\sigma = 4 \times 10^4\ \Omega^{-1}\ cm^{-1}$ (~6% that of bulk Ag), was obtained when Ag was deposited in the absence of gum arabic.

These morphologies result whether Ag is deposited on uniform films or porous microstructures (compare Figure 3A with Figure 2C). This suggests that the morphology is not affected by diffusion and mass-transport, even for the highly microporous structures shown here. This underscores the usefulness of the present method in that metal can be deposited with consistent morphology, regardless of variations in shape or microporosity across a structure. Additionally, conditions that favor deposition of Ag in the form of the smaller spheroidal nanocrystallites could be selected for applications that require uniform coatings. Atomic force microscopy (AFM) measurements of root-mean-squared roughness yielded values of approximately 5 nm for untreated uniform films, which implies that the polymer surface itself contributes negligibly to the observed morphology and surface roughness. For thick Ag layers (~100 nm), the morphologies are independent of whether nucleation sites are created by reducing bound Au(III) or directly attaching Au-NPs. AFM surface profilometry shows that the photopatterning and amination conditions used here generate a dense surface coverage of Au-NPs. Thus, the different morphologies do not appear to result from a surface-/seed-particle-directed effect, but rather from an inherent change in crystal plane growth kinetics.

Physical and chemical properties are now well-known to depend sensitively on nanoscale size and shape. To note just one example, rod-shaped noble metal NPs exhibit long-wavelength longitudinal plasmon resonances at visible wavelengths that are not produced by spherical particles of comparable diameter.[13] Given this, the process described here may also provide a route to new materials and devices whose ensemble properties can be tailored by changes in structure on both the microscale (determined by DLW) and nanoscale (determined by morphology of the deposited silver). Because the process selectively deposits conducting metal conformally onto the polymeric surface without altering the substrate, it provides a flexible means for creating 3D microstructures with metallic electrical or optical function based on scaffolds created with the high-performance polymer SU-8, that would be difficult or impossible to create by other pattering methods.

Acknowledgment. This work was supported by the ACS Petroleum Research Fund (Grant 42322-G5); the CREOL NSF-IGERT program (for A.T., Grant 0114418); and Coherent Lasers, Nikon Instruments, and Horiba-Jobin-Yvon, who are members of the CREOL Industrial Affiliates program, University of Central Florida. The authors thank Prof. Glenn Boreman and Mr. Guy Zummo for generously providing access to a four-point-probe instrument and the reviewers for their thoughtful and insightful comments.

Supporting Information Available: Epoxide resin and silvering bath formulations and processing conditions for multiphoton DLW and electroless deposition (PDF). This material is available free of charge via the Internet at http://pubs.acs.org.

CM0710812

(13) Link, S.; El-Sayed, M. A. *J. Phys. Chem. B* **1999**, *103*, 8410.